Biochemical and Biophysical Research Communications 591 (2022) 95–101

Contents lists available at ScienceDirect

Biochemical and Biophysical Research Communications

journal homepage: www.elsevier.com/locate/ybbrc

Roles of the SUMO-related enzymes, PIAS1, PIAS4, and RNF4, in DNA double-strand break repair by homologous recombination

Moe Moe Han [a], Miyako Hirakawa [b], Motohiro Yamauchi [c, *, 1], Naoki Matsuda [a, b, c]

[a] Graduate School of Biomedical Sciences, Nagasaki University, Nagasaki, 852-8523, Japan
[b] Center for Radiation Research and Education, Nagasaki University, Nagasaki, 852-8523, Japan
[c] Department of Radiation Biology and Protection, Atomic Bomb Disease Institute, Nagasaki University, Nagasaki, 852-8523, Japan

ARTICLE INFO

Article history:
Received 17 December 2021
Accepted 25 December 2021
Available online 30 December 2021

Keywords:
DNA double-strand break
Homologous recombination
Resection
Small ubiquitin-like modifier

ABSTRACT

Post-translational modification of proteins by small ubiquitin-like modifier (SUMO) is known to be involved in a variety of cellular events. This modification, called SUMOylation, is carried out by the E1 activating enzyme, the E2 conjugating enzyme, and multiple E3 ligases. Previous studies have demonstrated that the SUMO E3 ligases, protein inhibitors of activated STAT 1 (PIAS1) and 4 (PIAS4), and the SUMO-targeted ubiquitin ligase, RING finger protein 4 (RNF4), play important roles in the repair of DNA double-strand breaks (DSBs). However, the mechanism by which these SUMO-related enzymes promote DSB repair is still poorly understood. In the present study, we focused on homologous recombination (HR), the most accurate DSB repair pathway, and aimed to elucidate the mechanism by which PIAS1, PIAS4, and RNF4 promote HR. In γ-ray-irradiated normal human fibroblasts, DSB end resection and RAD51 loading, the two essential steps of HR, were significantly impaired by small interfering RNA (siRNA)-mediated depletion of PIAS1, PIAS4, or RNF4. The recruitment of BRCA1, a major HR factor, to DSB sites was reduced in cells depleted of these SUMO-related enzymes. Consistent with the role of BRCA1 in counteracting the p53-binding protein 1 (53BP1)-mediated resection blockade, 53BP1 depletion rescued the reduced resection and RAD51 loading in the cells depleted of PIAS1, PIAS4, or RNF4. Moreover, Rap1-interacting factor 1 (RIF1), a resection inhibitor downstream of 53BP1, became more abundant at DSBs when PIAS1, PIAS4, RNF4, or BRCA1 was depleted. Importantly, the concomitant depletion of BRCA1 with either one of the SUMO-related enzymes did not further increase RIF1 at DSBs, when compared to single depletion of BRCA1. Collectively, these results suggest that PIAS1, PIAS4, RNF4, and BRCA1 work epistatically to counteract 53BP1/RIF1-mediated resection blockade, thereby promoting resection.

1. Introduction

Genome integrity is constantly challenged by exogenous and endogenous factors, such as ionizing radiation, reactive oxygen species, and transcription [1–3]. Cells have evolved finely tuned mechanisms to repair DNA damage. DNA double-strand breaks (DSBs) are one of the most cytotoxic types of DNA damage. Failure or error in DSB repair can lead to cell death and chromosome rearrangement [4,5]. Thus, accurate repair of DSBs must be ensured to maintain genome integrity. Higher eukaryotes have two major pathways to repair DSBs: non-homologous end joining (NHEJ) and homologous recombination (HR) [6,7]. In NHEJ, DSB ends are first detected and bound by the Ku70/80 heterodimer [6,7]. Then, the Ku heterodimer recruits other NHEJ factors, such as DNA-PKcs, XRCC4, XLF, PAXX, and LIG4, and LIG4 ligates two DSB ends [6,7]. NHEJ can operate in any cell cycle phase [6,7]. In HR, DSB ends first undergo 5′–3′ resection, which is carried out by resection factors, such as MRE11/RAD50/NBS1/CtIP and EXO1/BLM/DNA2 [6,7]. The resultant 3′-overhanged single-stranded DNA (ssDNA) was coated with the replication protein A (RPA). Then, RPA on ssDNA was replaced with RAD51 recombinase. RAD51 helps ssDNA invade the duplex DNA molecules and search homology, thereby facilitating base-pairing with complementary sequences [6]. Thereafter, several distinct pathways can operate; however, in somatic cells, synthesis-dependent strand annealing is the predominant pathway, where RAD51-mediated invasion occurs only at one end of the two-ended

* Corresponding author.
E-mail address: yamauchi.motohiro.619@m.kyushu-u.ac.jp (M. Yamauchi).
[1] Present affiliation and contact information Hospital Campus Laboratory, Radioisotope Center, Central Institute of Radioisotope Science and Safety, Kyushu University, Fukuoka, 812–8582, Japan.

https://doi.org/10.1016/j.bbrc.2021.12.099
0006-291X/

Abbreviations

SUMO	small ubiquitin-like modifier
PIAS1	protein inhibitors of activated STAT 1
PIAS4	protein inhibitors of activated STAT 4
RNF4	RING finger protein 4
DSB	DNA double-strand break
NHEJ	non-homologous end-joining
HR	homologous recombination
siRNA	small interfering RNA

DSBs, with the other end not involved in the invasion [6]. HR operates mainly in late S and G_2 phase, when sister chromatids are available [6,7].

Small ubiquitin-like modifier (SUMO) is a protein of approximately 100 amino acids, which is used for a post-translational modification, called SUMOylation [8,9]. Although lower eukaryotes possess only one SUMO, higher eukaryotes have at least three SUMO isoforms (SUMO1–3) [9]. SUMOylation is carried out by the E1 activating enzyme, E2 conjugating enzyme, and E3 ligase [8,9]. While only a single E1 and E2 have been identified so far, there are multiple E3 ligases that determine the substrate specificity [8,9]. SUMOylation is known to affect several intracellular structures and events, including the formation of nucleoli and promyelocytic leukemia (PML) bodies, chromosomal structure, and phase separation [9]. Previous studies have demonstrated that SUMOylation is also involved in DSB repair. SUMO1 and SUMO2/3 are detected in chromatin containing DSBs [10,11]. The SUMO E3 ligases, protein inhibitors of activated STAT 1 (PIAS1) and 4 (PIAS4), promote both NHEJ and HR, and enhance cellular resistance to ionizing radiation [10]. Moreover, RING finger protein 4 (RNF4), a SUMO-targeted ubiquitin ligase, is recruited to DSB sites in a manner dependent on PIAS1 and PIAS4 [12]. Additionally, RNF4 is involved in both NHEJ and HR [12]. However, the mechanism by which PIAS1, PIAS4, and RNF4 facilitate DSB repair remains unclear.

In the present study, we focused on HR and aimed to elucidate the mechanism by which PIAS1, PIAS4, and RNF4 promote HR. We found that PIAS1, PIAS4, and RNF4 promote DSB end resection and RAD51 loading, which are the two critical steps of HR. Moreover, we obtained evidence that these SUMO-related enzymes and BRCA1 work epistatically to counteract the p53-binding protein 1 (53BP1)/Rap1-interacting factor 1 (RIF1)-mediated resection blockade.

2. Materials and methods

2.1. Cell culture and irradiation

BJ-hTERT cells (normal human foreskin fibroblasts immortalized with hTERT) were cultured in α-modified minimal essential medium (α-MEM) supplemented with 10% fetal bovine serum and 10 mM 4-(2-hydroxyethyl)-1-piperazineëthanesulfonic acid (HEPES). Cells were irradiated with ^{137}Cs γ-ray irradiator at a dose rate of 1 Gy/min.

2.2. Small interfering RNA (siRNA) transfection

Reverse transfection of siRNA was performed with Lipofectamine RNAiMAX (Thermo Fisher Scientific, MA, USA), according to the manufacturer's protocol, with some modifications. Briefly, siRNA and Lipofectamine RNAiMAX were diluted in Opti-MEM I (Thermo Fisher Scientific, MA, USA) and incubated for 10–20 min at room temperature (r.t.). During incubation, the cells were harvested by trypsinization and suspended in the medium. Then, the cell suspension (1×10^5 cells/mL) was mixed with diluted siRNA/Lipofectamine RNAiMAX and plated in a 35 mm dish. The final concentration of siRNA was 30 nM. siRNA transfection was performed twice on days 1 and 2. On Day 3 or 4, the cells were subjected to downstream experiments, such as irradiation and fixation. The siRNA sequences of PIAS1, PIAS4, and RNF4 are shown in Table S1.

2.3. Immunofluorescence

For immunofluorescence, the cells were plated onto coverslips in 35 mm dishes. To label the cells that had undergone DNA synthesis, they were treated with 10 μM 5-ethynyl-2′-deoxyuridine (EdU), a thymidine analogue, for 30 min before irradiation until fixation. For the detection of RPA, RAD51, and BRCA1 foci, the cells were pre-extracted with 0.2% Triton X-100 in phosphate-buffered saline (PBS) for 1 min followed by fixation with 3% paraformaldehyde/2% sucrose in PBS for 10 min at room temperature. For detection of RIF1 foci, the cells were fixed with 3% paraformaldehyde/2% sucrose in PBS for 10 min at r.t., followed by permeabilization with 0.2% Triton X-100 in PBS for 2.5 min. Primary antibodies were then incubated for 30 min at 37 °C, followed by incubation with Alexa Fluor 488- or 555-conjugated secondary antibodies for 30 min at 37 °C. The primary antibodies used for immunofluorescence are listed in Table S2. All antibodies were diluted in 2% bovine serum albumin (BSA) in PBS. After the secondary antibody reaction, samples were treated with the EdU detection solution (Alexa Fluor 647 azide in 100 mM Tris-HCl, 100 mM L-ascorbic acid, and 4 mM $CuSO_4$) for 30 min at r.t. in the dark. Then, coverslips were mounted onto glass slides with VectaShield containing 4′, 6-diamidino-2-phenylindole (DAPI) (Vector Laboratories, USA). Foci images were acquired using a confocal laser microscope (LSM800; Zeiss, Germany) with a 100× objective. Z stacks were taken at interval of 0.2–0.25 μm and maximal intensity projection images were obtained using ZEN 2.3 image analysis software (Zeiss, Germany).

2.4. Foci counting

In this study, we counted the foci of RPA, RAD51, BRCA1, and RIF1 in G_2 phase cells using a fluorescence microscope (Olympus, Japan). Since EdU (+) cells are S phase cells and centromere protein F (CENPF) (+) cells are S or G_2 phase cells, EdU (−)/CENPF(+) cells were regarded as G_2 phase cells.

2.5. Statistical analyses

Statistical analyses were performed using Prism 7 software (GraphPad Software, CA, USA). The two-tailed Mann–Whitney *U* test and Dunn's multiple comparison test were used to compare two or more populations, respectively. Statistical significance was set at $P < 0.05$.

3. Results

3.1. Roles of PIAS1, PIAS4, and RNF4 in DSB end resection

Previous studies have shown that PIAS1, PIAS4, and RNF4 are involved in HR, using the endonuclease (I-Sce I)-based reporter assay [10,12]. However, whether and how these SUMO-related enzymes promote HR of radiation-induced DSBs remain poorly understood. One of the essential steps in HR is DSB end resection [6,7]. Resection results in the formation of ssDNA, which is subsequently coated with RPA [6,7]. RPA assembly on ssDNA can be

visualized as RPA foci by immunofluorescence [13]. Thus, the RPA foci were used as an indicator of resection. Using RPA foci, we investigated whether PIAS1, PIAS4, and RNF4 promote resection. Since RPA can form foci in the S phase, even without exogenous DNA damaging stimuli, we analyzed RPA foci in the G_2 phase. To identify the G_2 phase, S phase cells were labeled with EdU, a thymidine analog, and S/G_2 phase cells were stained with CENPF, an S/G_2 phase marker [13]. EdU (−)/CENPF(+) cells were regarded as G_2 cells, and RPA foci in γ-ray-irradiated G_2 cells were counted. We found that siRNA-mediated depletion of PIAS1, PIAS4, or RNF4 significantly reduced the RPA foci (Fig. 1A–D, Supplementary Figs. S1A–C). The reduction of RPA foci by depletion of PIAS1, PIAS4, or RNF4 was similar and not significantly different between them (Supplementary Figs. S2A–B). These results suggest that PIAS1, PIAS4, and RNF4 promote DSB end resection in the G_2 phase.

3.2. Roles of PIAS1, PIAS4 and RNF4 in RAD51 loading

After resection, RPA bound to ssDNA is replaced by RAD51 [6,7]. RAD51 loading can also be visualized as RAD51 foci by immunofluorescence [14]. Thus, the roles of PIAS1, PIAS4, and RNF4 in RAD51 loading were examined using RAD51 foci. PIAS1, PIAS4, or RNF4 were depleted by siRNA, and RAD51 foci in G_2 phase were counted. We found that the number of RAD51 foci formed after γ-ray irradiation was significantly lower in the cells depleted of PIAS1, PIAS4 or RNF4 than in the mock-depleted cells (Fig. 1E–H, Supplementary Figs. S3A–C). The reduction was comparable between the cells depleted of PIAS1, PIAS4, or RNF4 (Supplementary Figs. S4A–B). These results indicate that PIAS1, PIAS4, and RNF4 facilitate RAD51 loading on resected DSBs in the G_2 phase.

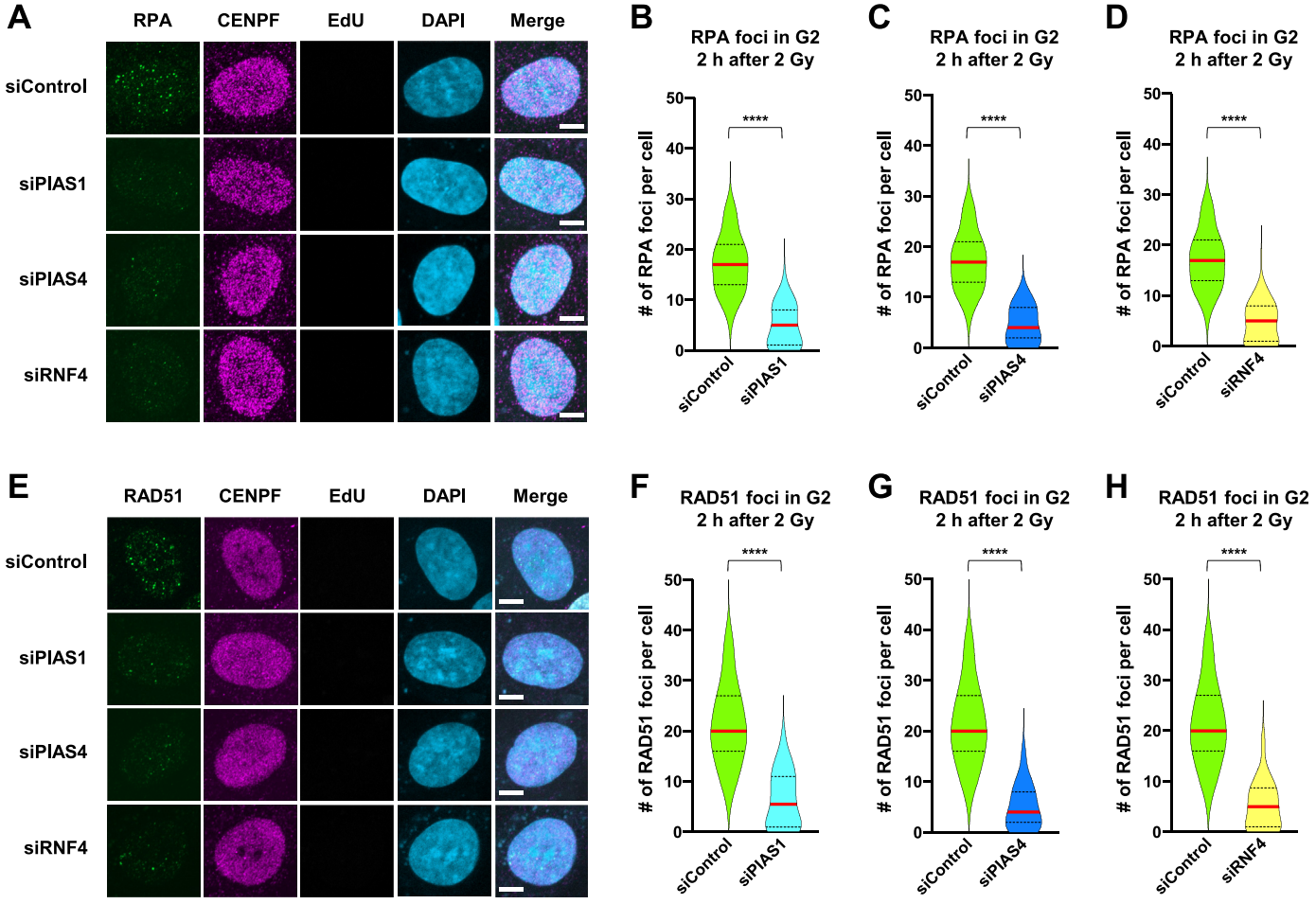

Fig. 1. Roles of the protein inhibitors of activated STAT 1 (PIAS1) and 4 (PIAS4), and RING finger protein 4 (RNF4) in DNA double-strand break (DSB) end resection and RAD51 loading. (A) Representative images of the replication protein A (RPA) foci in mock-depleted cells (siControl) or cells depleted of PIAS1, PIAS4, or RNF4 (siPIAS1, siPIAS4, and siRNF4). BJ-hTERT cells were transfected twice with the indicated small interfering RNA (siRNA). Two to three days after the 1st siRNA transfection, the cells were irradiated with 2 Gy and then fixed 2 h later. Then, these cells were subjected to immunofluorescence of RPA/centromere protein F (CENPF) and 5-ethynyl-2′-deoxyuridine (EdU) detection. The figure shows RPA foci in CENPF(+)/EdU(−) G_2 phase cells. Scale bar, 5 μm. (B) (C) (D) Numbers of RPA foci in mock-depleted cells (siControl) or the cells depleted of PIAS1 (B), PIAS4 (C), or RNF4 (D). The samples were prepared as described in (A). The graph shows a violin plot of the number of RPA foci in BJ-hTERT cells transfected with siControl (B–D), siPIAS1 (B), siPIAS4 (C), or siRNF4 (D). (E) Representative images of RAD51 foci in mock-depleted cells (siControl) or the cells depleted of PIAS1, PIAS4, or RNF4 (siPIAS1, siPIAS4, and siRNF4). BJ-hTERT cells were transfected with the indicated siRNA. Two to three days after siRNA transfection, the cells were irradiated with 2 Gy and then fixed 2 h later. Then, these cells were subjected to immunofluorescence of RAD51/CENPF and EdU detection. The figure shows RAD51 foci in CENPF(+)/EdU(−) G_2 phase cells. Scale bar, 5 μm. (F) (G) (H) Numbers of RAD51 foci in mock-depleted cells (siControl) or the cells depleted of PIAS1 (F), PIAS4 (G), or RNF4 (H). The samples were prepared as described in (E). The graph shows a violin plot of the number of RAD51 foci in BJ-hTERT cells transfected with siControl (F–H), siPIAS1 (F), siPIAS4 (G), or siRNF4 (H). Red solid lines and black dotted lines indicate the medians and quartiles of the number of foci, respectively. The foci were counted in 50 G_2 cells in one experiment, and two independent experiments were done for each sample (i.e., foci were counted in a total of 100 cells for each sample). ****P < 0.0001. (For interpretation of the references to colour in this figure legend, the reader is referred to the Web version of this article.)

3.3. Roles of PIAS1, PIAS4, and RNF4 in the recruitment of BRCA1 to DSBs

BRCA1 plays important roles in several steps of HR, including resection and RAD51 loading [15]. Therefore, we next investigated whether PIAS1, PIAS4, and RNF4 have some relationship with BRCA1. Upon DSBs, BRCA1 is recruited to DSB sites, which can be visualized as BRCA1 foci by immunofluorescence [16]. Thus, we examined the impact of PIAS1, PIAS4, and RNF4 on the foci formation of BRCA1 after γ-ray irradiation. We found that the depletion of PIAS1, PIAS4 or RNF4 significantly reduced the number of BRCA1 foci in the cells irradiated in the G_2 phase (Fig. 2A–C, Supplementary Figs. S5A–C). The reduction of BRCA1 foci by the depletion of PIAS1, PIAS4, and RNF4 was similar (Supplementary Figs. S6A–B). Together, these results suggest that PIAS1, PIAS4, and RNF4 promote BRCA1 recruitment to DSBs.

3.4. PIAS1, PIAS4, and RNF4 counteract 53BP1-mediated resection blockade

BRCA1 facilitates resection by counteracting 53BP1-mediated resection blockade [15]. The finding that PIAS1, PIAS4, and RNF4 promoted BRCA1 foci formation (Fig. 2) led us to hypothesize that these factors may help BRCA1 antagonize 53BP1. To test this hypothesis, we investigated whether the requirement of PIAS1, PIAS4, and RNF4 for resection was reduced by 53BP1 depletion. As shown in Fig. 3A, 53BP1 depletion significantly increased the number of RPA foci in PIAS1-depleted cells (cf. siPIAS1 and siPIAS1 + si53BP1). Similarly, under the condition where PIAS4 or RNF4 was depleted, RPA foci were increased by 53BP1 depletion (Fig. 3B and C; cf. siPIAS4 and siPIAS4 + si53BP1; siRNF4 and siRNF4 + si53BP1). These results indicated that the requirement of PIAS1, PIAS4, and RNF4 for resection was reduced when 53BP1 was depleted. Since increased resection should restore RAD51 loading, we next examined the effect of 53BP1 depletion on RAD51 foci in the cells depleted of PIAS1, PIAS4, or RNF4. As shown in Fig. 3D, 53BP1 depletion significantly increased the RAD51 foci number in PIAS1-depleted cells (cf. siPIAS1 and siPIAS1 + si53BP1). Rescue of RAD51 foci number by 53BP1 depletion was also observed in PIAS4- and RNF4-depleted cells (Fig. 3E and F; cf. siPIAS4 and siPIAS4 + si53BP1; siRNF4 and siRNF4 + si53BP1). These results suggest that 53BP1 depletion bypassed the need for the SUMO-related enzymes for RAD51 loading. Collectively, the results in Fig. 3 indicate that PIAS1, PIAS4, and RNF4 counteract 53BP1-mediated resection blockade.

3.5. PIAS1, PIAS4, and RNF4 limit RIF1 recruitment to DSB sites

RIF1 protein functions as a resection inhibitor downstream of 53BP1 [6,7,17]. RIF1 is recruited to DSBs in a manner dependent on 53BP1 phosphorylation [18]. A previous study demonstrated that BRCA1 promotes dephosphorylation of 53BP1 and limits RIF1 assembly at DSBs, thereby facilitating resection [13]. Since PIAS1, PIAS4, and RNF4 promoted BRCA1 recruitment to DSBs (Fig. 2), we speculated that these SUMO-related enzymes help BRCA1 control RIF1 recruitment to DSBs. Therefore, we examined the role of the SUMO-related enzymes in RIF1 assembly at DSBs. For this purpose, we examined RIF1 foci, which indicate RIF1 localization at DSB sites [13,18]. The number of RIF1 foci was quantified at 30 m and 4 h after 1 Gy of γ-ray irradiation (Fig. 4). We found that depletion of PIAS1, PIAS4, RNF4, and BRCA1 similarly increased the number of RIF1 foci, both at 30 m and 4 h after IR (Fig. 4A–F). Moreover, the concomitant depletion of BRCA1 and either one of the SUMO-related enzymes did not further increase the number of RIF1 foci, indicating that BRCA1 and these enzymes work epistatically to limit RIF1 recruitment to DSBs (Fig. 4A–F).

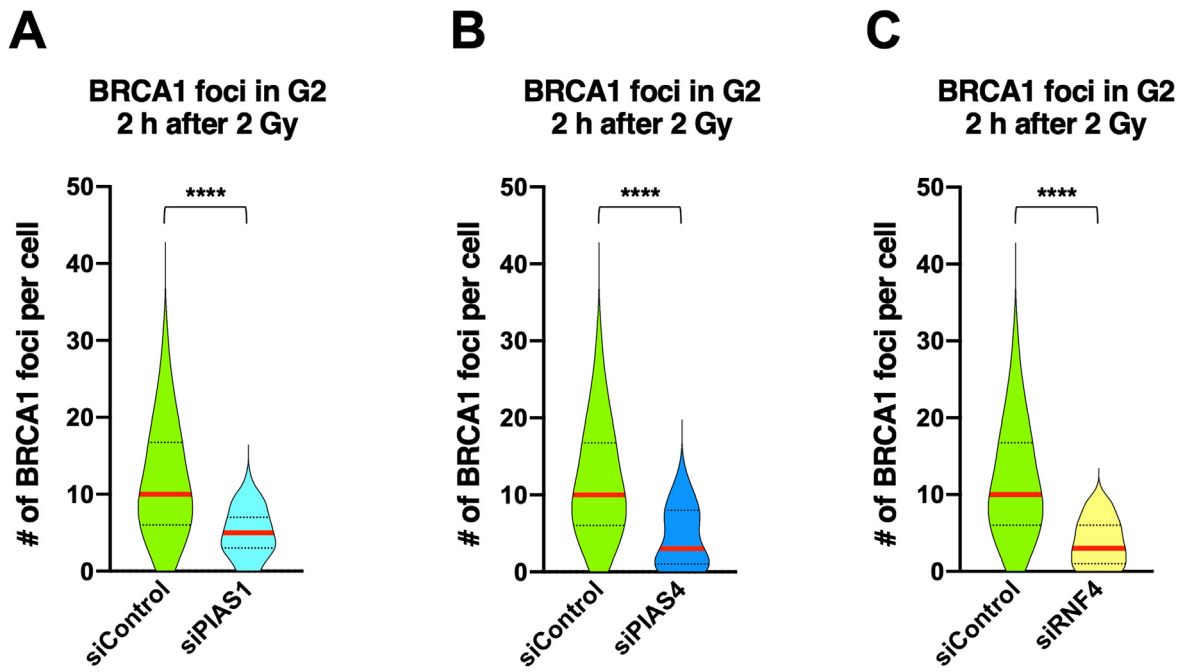

Fig. 2. Role of PIAS1, PIAS4, and RNF4 in BRCA1 recruitment to DSBs. (A) (B) (C) Numbers of BRCA1 foci in mock-depleted cells (siControl) or cells depleted of PIAS1 (A), PIAS4 (B), or RNF4 (C). BJ-hTERT cells were transfected with the indicated siRNA. Two to three days after siRNA transfection, the cells were irradiated with 2 Gy and then fixed 2 h later. Then, these cells were subjected to immunofluorescence of BRCA1/CENPF and EdU detection. The graph shows the violin plot of the numbers of BRCA1 foci in BJ-hTERT cells transfected with siControl (A–C), siPIAS1 (A), siPIAS4 (B), or siRNF4 (C). Red solid lines and black dotted lines indicate the medians and quartiles of the numbers of foci, respectively. The foci were counted in 50 G_2 cells in one experiment, and two independent experiments were done for each sample (i.e., foci were counted in a total of 100 cells for each sample). ****P < 0.0001. (For interpretation of the references to colour in this figure legend, the reader is referred to the Web version of this article.)

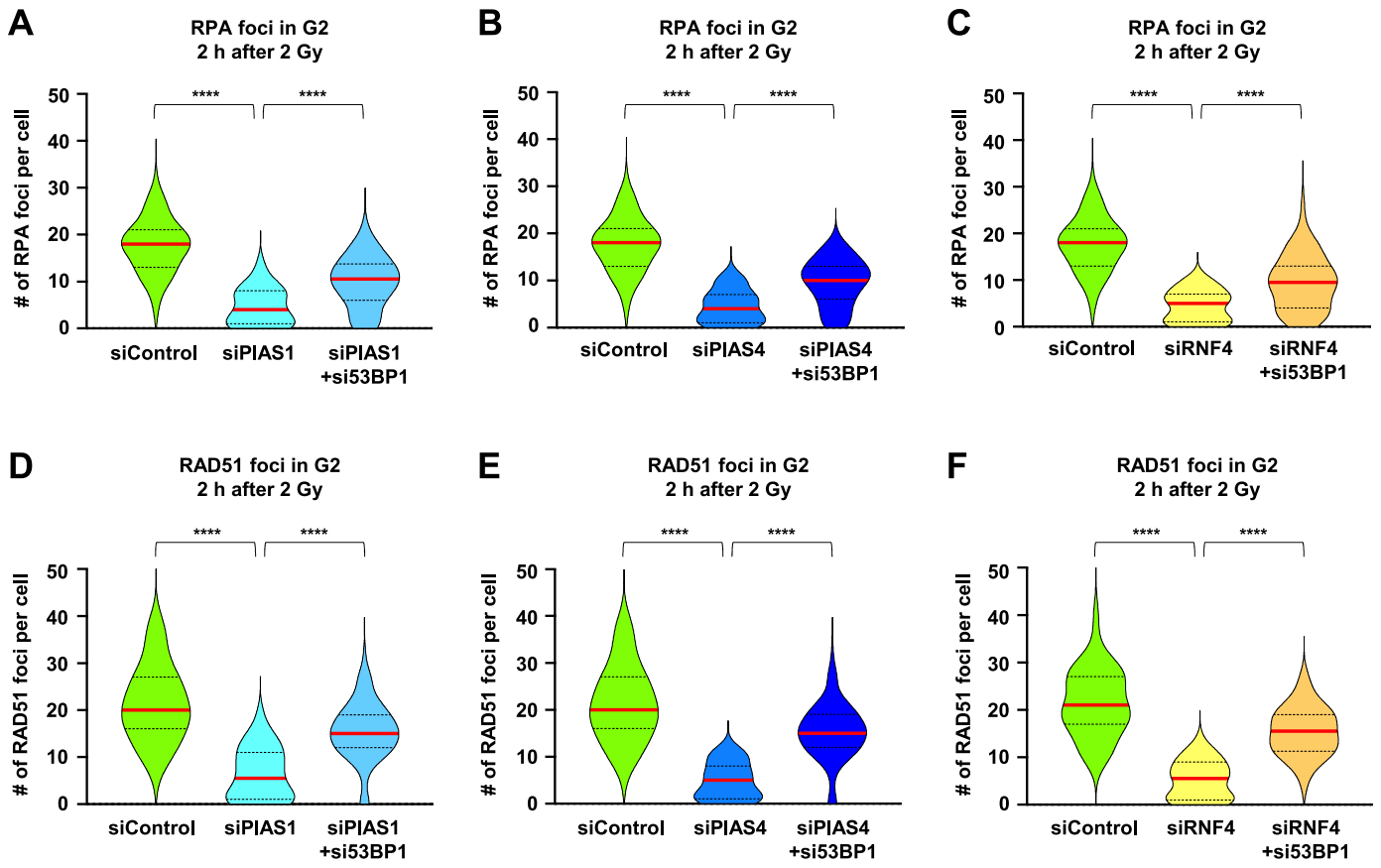

Fig. 3. PIAS1, PIAS4, and RNF4 counteract the p53-binding protein 1 (53BP1)-mediated resection blockade. (A) (B) (C) Numbers of RPA foci in mock-depleted cells (siControl), cells singly depleted of PIAS1 (A), PIAS4 (B), or RNF4 (C), or cells doubly depleted of PIAS1 + 53BP1 (A), PIAS4 + 53BP1 (B), or RNF4 + 53BP1 (C). BJ-hTERT cells were transfected with the indicated siRNA(s). Two to three days after siRNA transfection, the cells were irradiated with 2 Gy and then fixed 2 h later. Then, these cells were subjected to immunofluorescence of RPA/CENPF and EdU detection. The graph shows the violin plot of the numbers of RPA foci in BJ-hTERT cells transfected with siControl (A–C), siPIAS1 (A), siPIAS1 + si53BP1 (A), siPIAS4 (B), siPIAS4 + si53BP1 (B), siRNF4 (C), or siRNF4 + si53BP1 (C). (D) (E) (F) Numbers of RAD51 foci in mock-depleted cells (siControl), cells singly depleted of PIAS1 (D), PIAS4 (E), or RNF4 (F), or cells doubly depleted of PIAS1 + 53BP1 (D), PIAS4 + 53BP1 (E), or RNF4 + 53BP1 (F). BJ-hTERT cells were transfected with the indicated siRNA(s). Two to three days after siRNA transfection, the cells were irradiated with 2 Gy and then fixed 2 h later. Then, these cells were subjected to immunofluorescence of RAD51/CENPF and EdU detection. The graph shows the violin plot of the numbers of RAD51 foci in BJ-hTERT cells transfected with siControl (D–F), siPIAS1 (D), siPIAS1 + si53BP1 (D), siPIAS4 (E), siPIAS4 + si53BP1 (E), siRNF4 (F), or siRNF4 + si53BP1 (F). Red solid lines and black dotted lines indicate the medians and quartiles of the numbers of foci, respectively. The foci were counted in 50 G_2 cells in one experiment, and two independent experiments were done for each sample (i.e., foci were counted in a total of 100 cells for each sample). ****P < 0.0001. (For interpretation of the references to colour in this figure legend, the reader is referred to the Web version of this article.)

4. Discussion

In this study, we investigated the roles of the two SUMO E3 ligases (PIAS1 and PIAS4) and the SUMO-targeted ubiquitin ligase (RNF4) in HR of radiation-induced DSBs in G_2 phase. We showed that the depletion of PIAS1, PIAS4, and RNF4 suppressed foci formation of RPA, RAD51, and BRCA1. Moreover, the depletion of these SUMO-related enzymes increased the foci number of RIF1, a resection inhibitor working downstream of 53BP1, at DSB sites.

Galanty et al. reported that RPA recruitment to the track of DSB-generating laser was decreased in PIAS1-, or PIAS4-depleted cells [10]. Yin et al. showed that RPA70 recruitment to endonuclease (AsiSI)-induced DSBs was diminished by RNF4 depletion [19]. Thus, these studies and ours suggest that PIAS1, PIAS4, and RNF4 generally promote resection of DSBs generated by different kinds of DSB inducers. Regarding RAD51, two groups reported that RAD51 recruitment to laser track was compromised in RNF4-depleted cells [12,19]. We found that the depletion of PIAS1 or PIAS4 reduced the number of RAD51 foci similarly to RNF4 depletion (Supplementary Fig. S4). Given that RNF4 recruitment to DNA damage is dependent on PIAS1 and PIAS4 [12], it is likely that PIAS1 and PIAS4 promote RAD51 loading through RNF4.

Regarding BRCA1, previous studies reported that BRCA1 recruitment to DSBs induced by laser or hydroxyurea was decreased by the depletion of PIAS1 or PIAS4 [10,11]. Our results showed that RNF4 depletion impaired BRCA1 foci formation similarly to the depletion of PIAS1 or PIAS4 (Supplementary Fig. S6). Considering the above studies and ours, it is suggested that PIAS1 and PIAS4 promote BRCA1 recruitment via RNF4.

We found that reduction of RPA-, or RAD51 foci in PIAS1-, PIAS4, or RNF4-depleted cells was partially rescued by concomitant depletion of 53BP1 (Fig. 3). Moreover, the depletion of PIAS1, PIAS4, or RNF4 promoted foci formation of RIF1 (Fig. 4). These results indicate that PIAS1, PIAS4, and RNF4 are all involved in antagonizing 53BP1/RIF1-mediated resection blockade. This is supported by the previous study reporting that resolution of RIF1 foci after bleomycin treatment was delayed in PIAS4-depleted cells [20]. We propose that these SUMO-related enzymes counteract 53BP1/RIF1-mediated resection blockade through BRCA1, because (1) these enzymes promoted BRCA1 recruitment to DSBs (Fig. 2), (2) RIF1 foci were increased similarly by BRCA1-depletion and the depletion of these enzymes (Fig. 4), (3) the concomitant depletion of BRCA1 and any of PIAS1, PIAS4, or RNF4 did not further increase RIF1 foci, compared to the single depletion of BRCA1 (Fig. 4). To our best

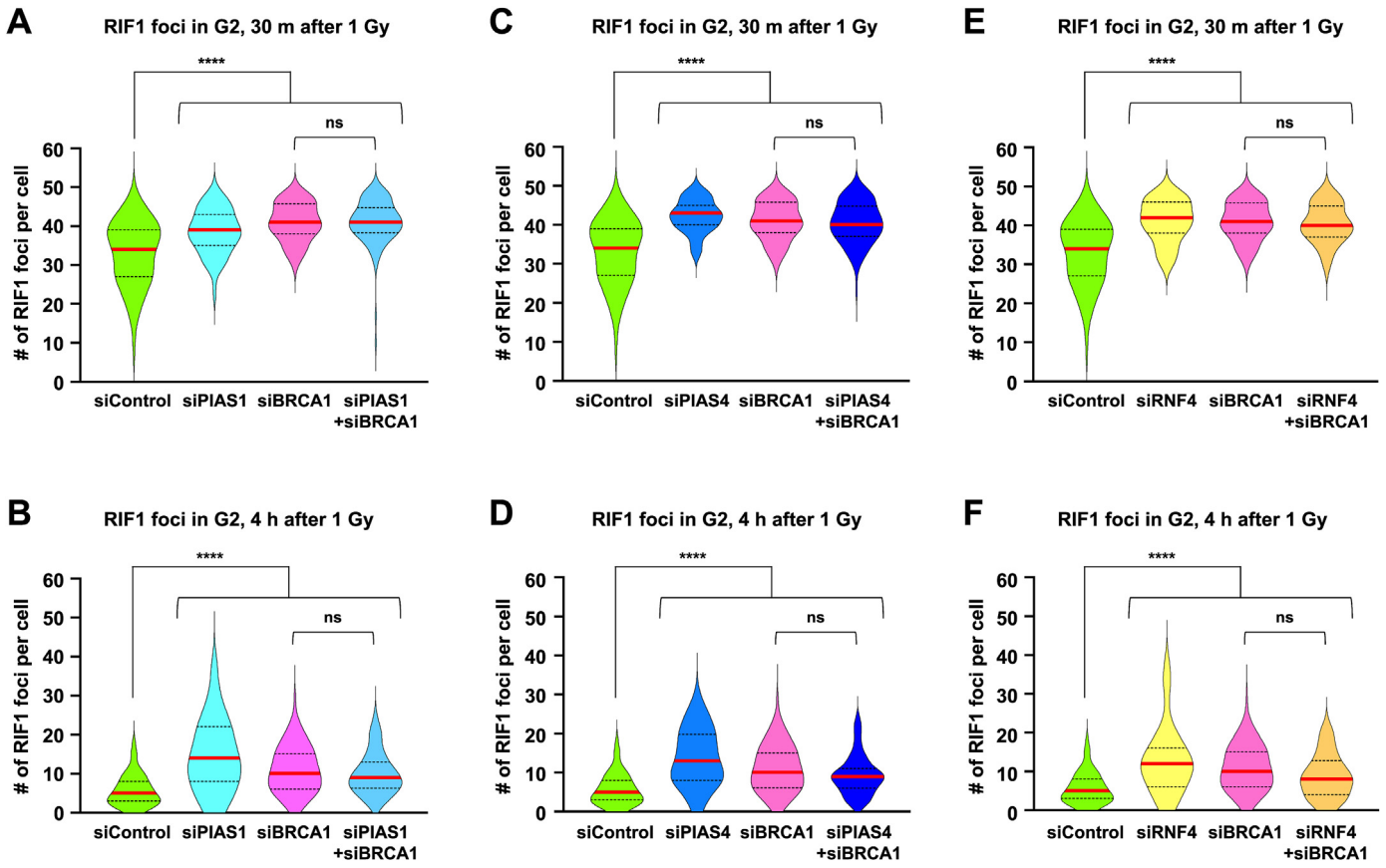

Fig. 4. PIAS1, PIAS4, and RNF4 limit Rap1-interacting factor 1 (RIF1) recruitment to DSB sites. (A–F) Numbers of RIF1 foci in mock-depleted cells (siControl), cells singly depleted of PIAS1, PIAS4, or RNF4, or cells doubly depleted of PIAS1 + BRCA1, PIAS4 + BRCA1, or RNF4 + BRCA1. BJ-hTERT cells were transfected with the indicated siRNA(s). Two to three days after siRNA transfection, the cells were irradiated with 1 Gy and then fixed 30 m (A, C, E) or 4 h (B, D, F) later. Then, these cells were subjected to immunofluorescence of RIF1/CENPF and EdU detection. The graphs show the violin plot of the numbers of RIF1 foci in BJ-hTERT cells transfected with siControl (A–F), siBRCA1 (A–F), siPIAS1 (A, B), siPIAS1 + siBRCA1 (A, B), siPIAS4 (C, D), siPIAS4 + siBRCA1 (C, D), siRNF4 (E, F), or siRNF4 + siBRCA1 (E, F). Red solid lines and black dotted lines indicate the medians and quartiles of the numbers of foci, respectively. The foci were counted in 50 G_2 cells in one experiment, and two independent experiments were done for each sample (i.e., foci were counted in a total of 100 cells for each sample). ****P < 0.0001; ns, not significant. (For interpretation of the references to colour in this figure legend, the reader is referred to the Web version of this article.)

knowledge, this is the first study reporting epistatic relationship between BRCA1 and PIAS1/PIAS4/RNF4 in limiting RIF1 recruitment to DSBs.

In summary, we showed that PIAS1, PIAS4, and RNF4 promoted resection and RAD51 loading, the two critical steps in HR. Our results suggest that these SUMO-related enzymes help BRCA1 counteract 53BP1/RIF1-mediated resection blockade, thereby facilitating resection.

Author contributions

M.Y. conceived and designed the study and prepared the manuscript. M.M.H. performed all experiments and statistical analyses. M.H. performed the preliminary immunofluorescence experiments. N.M. supervised the study.

Funding

This work was supported by Grants-in-Aid for Scientific Research (KAKENHI) from the Japan Society for the Promotion of Science [grant number JP18K11645 to M.Y.] and the Network-type Joint Usage/Research Center for Radiation Disaster Medical Science.

Declaration of competing interest

None declared.

Acknowledgements

We would like to thank all members of the Matsuda Lab (Department of Radiation Biology and Protection, Atomic Bomb Disease Institute, Nagasaki University) for their help.

Appendix A. Supplementary data

Supplementary data to this article can be found online at https://doi.org/10.1016/j.bbrc.2021.12.099

References

[1] J.F. Ward, DNA damage produced by ionizing radiation in mammalian cells, Identities, mechanisms of formation, and reparability, Prog. Nucleic Acid Res. Mol. Biol. 35 (1988) 95–125, https://doi.org/10.1016/S0079-6603(08)60611-X.
[2] N.R. Jena, DNA damage by reactive species: mechanisms, mutation and repair, J. Biosci. 37 (2012) 503–517, https://doi.org/10.1007/s12038-012-9218-2.
[3] H. Gaillard, A. Aguilera, Transcription as a Threat to genome integrity, Annu. Rev. Biochem. 85 (2016) 291–317, https://doi.org/10.1146/annurev-biochem-060815-014908.
[4] R. Ceccaldi, B. Rondinelli, A.D. D'Andrea, Repair pathway Choices and Consequences at the double-strand break, Trends Cell Biol 26 (2016) 52–64, https://

doi.org/10.1016/j.tcb.2015.07.009.
[5] M. Yamauchi, Mechanisms underlying the suppression of chromosome rearrangements by ataxia-telangiectasia mutated, Genes 12 (2021) 1232.
[6] R. Scully, A. Panday, R. Elango, N.A. Willis, DNA double-strand break repair pathway choice in somatic mammalian cells, Nat. Rev. Mol. Cell Biol. 20 (2019) 698–714, https://doi.org/10.1038/s41580-019-0152-0.
[7] A. Shibata, P.A. Jeggo, DNA double-strand break repair in a cellular context, Clin. Oncol. 26 (2014) 243–249, https://doi.org/10.1016/j.clon.2014.02.004.
[8] N. Dhingra, X. Zhao, Intricate SUMO-based control of the homologous recombination machinery, Genes Dev. 33 (2019) 1346–1354. http://www.genesdev.org/cgi/doi/10.1101/gad.328534.119.
[9] X. Zhao, SUMO-mediated Regulation of nuclear Functions and signaling processes, Mol. Cell. 71 (2018) 409–418, https://doi.org/10.1016/j.molcel.2018.07.027.
[10] Y. Galanty, R. Belotserkovskaya, J. Coates, S. Polo, K.M. Miller, S.P. Jackson, Mammalian SUMO E3-ligases PIAS1 and PIAS4 promote responses to DNA double-strand breaks, Nature 462 (2009) 935–939, https://doi.org/10.1038/nature08657.
[11] J.R. Morris, C. Boutell, M. Keppler, R. Densham, D. Weekes, A. Alamshah, L. Butler, Y. Galanty, L. Pangon, T. Kiuchi, T. Ng, E. Solomon, The SUMO modification pathway is involved in the BRCA1 response to genotoxic stress, Nature 462 (2009) 886–890, https://doi.org/10.1038/nature08593.
[12] Y. Galanty, R. Belotserkovskaya, J. Coates, S.P. Jackson, RNF4, a SUMO-targeted ubiquitin E3 ligase, promotes DNA double-strand break repair, Genes Dev 26 (2012) 1179–1195. http://www.genesdev.org/cgi/doi/10.1101/gad.188284.112.
[13] M. Isono, A. Niimi, T. Oike, Y. Hagiwara, H. Sato, R. Sekine, Y. Yoshida, S.Y. Isobe, C. Obuse, R. Nishi, E. Petricci, S. Nakada, T. Nakano, A. Shibata, BRCA1 directs the repair pathway to homologous recombination by promoting 53BP1 dephosphorylation, Cell Rep. 18 (2017) 520–532, https://doi.org/10.1016/j.celrep.2016.12.042.
[14] S. Tashiro, J. Walter, A. Shinohara, N. Kamada, T. Cremer, Rad51 accumulation at sites of DNA damage and in postreplicative chromatin, J. Cell Biol. 150 (2000) 283–291, https://doi.org/10.1083/jcb.150.2.283.
[15] M. Tarsounas, P. Sung, The antitumorigenic roles of BRCA1-BARD1 in DNA repair and replication, Nat. Rev. Mol. Cell Biol. 21 (2020) 284–299, https://doi.org/10.1038/s41580-020-0218-z.
[16] Y. Hu, R. Scully, B. Sobhian, A. Xie, E. Shestakova, D.M. Livingston, RAP80-directed tuning of BRCA1 homologous recombination function at ionizing radiation-induced nuclear foci, Genes Dev. 25 (2011) 685–700. http://www.genesdev.org/cgi/doi/10.1101/gad.2011011.
[17] D. Setiaputra, D. Durocher, Shieldin - the protector of DNA ends, EMBO Rep. 20 (2019), e47560, https://doi.org/10.15252/embr.201847560.
[18] C. Escribano-Díaz, A. Orthwein, A. Fradet-Turcotte, M. Xing, J.T.F. Young, J. Tkáč, M.A. Cook, A.P. Rosebrock, M. Munro, M.D. Canny, D. Xu, D. Durocher, A cell cycle-dependent regulatory circuit Composed of 53BP1-RIF1 and BRCA1-CtIP controls DNA repair pathway choice, Mol. Cell. 49 (2013) 872–883, https://doi.org/10.1016/j.molcel.2013.01.001.
[19] Y. Yin, A. Seifert, J.S. Chua, J.F. Maure, F. Golebiowski, R.T. Hay, SUMO-targeted ubiquitin E3 ligase RNF4 is required for the response of human cells to DNA damage, Genes Dev. 26 (2012) 1196–1208, https://doi.org/10.1101/gad.189274.112.
[20] R. Kumar, C.C. Fang, Dynamics of RIF1 SUMOylation is regulated by PIAS4 in the maintenance of Genomic Stability, Sci. Rep. 7 (2017) 17367, https://doi.org/10.1038/s41598-017-16934-w.